Geophysical Research Letters

RESEARCH LETTER
10.1029/2018GL079283

Key Points:
- The Mejillones Peninsula presents variability in the distributions of seismicity, swarms, and repeaters
- High V_P/V_S values indicate zones rich in fluids, correlated with the Mejillones fracture zone and permeable lithologies
- Areas rich in fluids control the seismogenic behavior of the plate interface beneath the Mejillones Peninsula

Supporting Information:
- Supporting Information S1

Correspondence to:
F. Pasten-Araya,
fpa007@ucn.cl

Citation:
Pasten-Araya, F., Salazar, P., Ruiz, S., Rivera, E., Potin, B., Maksymowicz, A., et al. (2018). Fluids along the plate interface influencing the frictional regime of the Chilean subduction zone, northern Chile. *Geophysical Research Letters*, *45*, 10,378–10,388. https://doi.org/10.1029/2018GL079283

Received 20 JUN 2018
Accepted 19 SEP 2018
Accepted article online 21 SEP 2018
Published online 11 OCT 2018

©2018. American Geophysical Union. All Rights Reserved.

Fluids Along the Plate Interface Influencing the Frictional Regime of the Chilean Subduction Zone, Northern Chile

F. Pasten-Araya[1,2], P. Salazar[1,2], S. Ruiz[3], E. Rivera[3], B. Potin[4], A. Maksymowicz[3], E. Torres[1,2], J. Villarroel[1,2], E. Cruz[1,2], J. Valenzuela[1,2], D. Jaldín[1], G. González[1,2], W. Bloch[5], P. Wigger[5], and S. A. Shapiro[5]

[1]Geology Department, Universidad Católica del Norte, Antofagasta, Chile, [2]Natural Research Center for Integrated Natural Disasters Management (CIGIDEN), Antofagasta, Chile, [3]Geophysics Department, Universidad de Chile, Santiago, Chile, [4]Centro Sismológico Nacional, Universidad de Chile, Santiago, Chile, [5]Fachrichtung Geophysik, Freie Universität Berlin, Berlin, Germany

Abstract The plate interface beneath the Mejillones Peninsula in Northern Chile is characterized by anomalous seismogenic behaviors, with seismic and aseismic slip, and low coupling values. We analyze this zone through the seismicity pattern and a 3-D tomography model. We identify high V_P/V_S values within the oceanic crust and in the lower continental crust, which we interpret as hydrated zones rich in fluids. These zones are correlated with the Mejillones fracture zone and with highly permeable lithologies of the lower continental crust, which allow a greater accumulation of fluids at the plate interface beneath the Mejillones Peninsula. Additionally, these areas exhibit a high rate of seismicity and concentrated swarms and repeaters. We propose that the presence of fluids controls the anomalous seismogenic behavior along the plate interface beneath the Mejillones Peninsula.

Plain Language Summary The interplate zone beneath Mejillones Peninsula (MP), northern Chile, presents an anomalous seismogenic behavior with aseismic pulses, low coupling values, and acting as a seismic barrier for earthquakes occurred in adjacent areas. We believe that this anomalous behavior is due to the presence of fluids in the interplate zone under the MP. To corroborate this, we study the seismicity recorded by a local seismological network and constructed a tomographic velocity model. Our results show that within the oceanic crust and in the lower continental crust exist the presence of fluids that concentrates to the north and center of the MP, which correlate with the presence of the Mejillones fracture zone and with more fractured and permeable lithologies of the continental crust. This situation changes to the south of the MP where fluid concentration is lower. This is the first detailed attempt to characterize the role of fluids in the rheology of barriers within subduction zones and to distinguish geological controls on the fluid distribution. We believe that this type of study is fundamental for facilitating future prospective analysis of earthquake distributions and conducting hazard assessments.

1. Introduction

The Chilean megathrust area, which accommodates many large-magnitude earthquakes (Mw > 8), exhibits a high seismicity rate. The subduction of the Nazca plate beneath the South American plate in northern Chile has produced several large-magnitude subduction earthquakes including the 1877 M_W ~ 8.5 earthquake (Comte & Pardo, 1991; Ruiz & Madariaga, 2018), the 1995 M_W 8.1 Antofagasta earthquake (Delouis et al., 1997), the 2007 M_W 7.7 Tocopilla earthquake (Delouis et al., 2009; Peyrat et al., 2010), and the 2014 M_W 8.2 Iquique earthquake (González et al., 2015; Ruiz et al., 2014; Schurr et al., 2014). The plate interface zone is geologically heterogeneous and the lateral extent of earthquake rupture usually stops at a seismic barrier where the slip deficit is reduced by many factors including the presence of fluids, which play a major role in the frictional behavior by controlling both the earthquake location and the seismicity rate (Audet & Schwartz, 2013; Schlaphorst et al., 2016). This aspect is important in subduction zones where earthquake generation is largely controlled by fluids released from prograding metamorphic reactions in the incoming oceanic lithosphere (Nishikawa & Ide, 2015; Poli et al., 2017). Lateral variations in the fluid concentration can be determined by using V_P and V_P/V_S seismic tomography, which is fundamental to understanding seismic patterns, and seismic segmentation and determining the frictional behavior in subduction zones.

In this contribution we try to understand the role of fluids in a section of the Chilean subduction zone located beneath the Mejillones Peninsula (MP) in northern Chile. The MP is considered a geomorphic anomaly corresponding to an uplifted block of the coastal platform. The northern and central subduction zone of the MP is associated with the Mejillones fracture zone (MFZ), which corresponds to a slab age discontinuity observed as a northwest magnetic lineament in the Nazca plate (Figure 1; Maksymowicz, 2015). The last two earthquakes that occurred in the area adjacent to the MP did not cross the interplate contact beneath the MP (Fuenzalida et al., 2013; Schurr et al., 2012). Aseismic slip occurred after the 1995 Mw 8.1 Antofagasta earthquake, with a total slip of 1.2 m (Pritchard & Simons, 2006). Furthermore, geodetic models show that the interplate locking in this section is reduced in comparison with adjacent subduction segments both to the north and to the south (Bejar-Pizarro et al., 2013; Metois et al., 2016). These conclusions strongly suggest that this section of the Chilean subduction zone exhibits behavior representative of a seismic barrier. We hypothesize that this barrier behavior of the interplate contact beneath the MP is controlled by rich fluids at the plate interface. To solve this problem, we deployed a short-period network in the MP to characterize the intraslab and interplate seismicity. Furthermore, we built a detailed 3-D tomography model and characterized the focal mechanisms of 1,248 events to characterize the stress regime in the subducting slab and along the subduction fault zone. This is the first detailed attempt to characterize the role of fluids in the rheology of barriers within subduction zones and to distinguish geological controls on the fluid distribution. We believe that this type of study is fundamental for facilitating future prospective analyses of earthquake distributions and conducting hazard assessments.

2. Data and Methods

We deployed a dense temporary seismic network in the vicinity of the MP, consisting of 24 short-period three-component seismometers (1 Hz MARK L4-3-D with EDPR6-24 data logger), that provided continuous records with a sampling rate of 200 Hz. This temporary network was registered continuously from July 2013 to September 2015 (Salazar et al., 2013). We also used the four broadband stations of the permanent Integrated Plate Boundary Observatory Chile (IPOC, 2006) network that were closest to the MP (Figure 1b).

2.1. Seismic Catalog

This first stage consisted of the construction of the seismic catalog. We manually searched the continuous records for events beneath the MP, following which a total of 5,727 events were found. To obtain the locations of these events, we manually determined the arrival times of the *P* and *S* waves using the SEISAN program (Havskov & Ottemöller, 2000). Using this program, we also calculated the local magnitude and polarity of each *P* wave to determine the associated focal mechanisms. Of the 5,727 identified events, it was possible to obtain the arrival times of 4,642 events. The remaining events were discarded due to high levels of noise in the waveforms. Then we determined the locations of the events with the arrival times, we used the NonLinLoc program (Lomax et al., 2000) using a 1-D velocity model (Husen et al., 1999). Later, to improve the accuracy of the locations, we used the double-difference relocation program (HypoDD; Waldhauser & Ellsworth, 2000) using the same velocity model. The resulting catalog is composed of 2,217 events, whose magnitudes vary in the range of $0.5 < M_L < 5.4$, with a completeness magnitude (M_C) of approximately 1.8 and an estimated depth error of less than 1.3 km (supporting information Figures S1 to S3).

From this final catalog, we determined the focal mechanisms of those events where it was possible to interpret the polarities (i.e., dilation or compression) of the *P* waves and the SV/P, SH/P, and SH/SV amplitude ratios. The polarities were read on the vertical component of the seismograms from each station. The FOCMEC program (Snoke et al., 1984) was used to compute the focal mechanisms of events that had more than seven polarities. Ultimately, we were able to obtain a total of 1,248 focal mechanisms.

2.2. 3-D Tomography Model

To construct the tomography model we used the INSIGHT code package (Potin, 2016). The model consists of a set of V_P, V_S, and V_P/V_S values given for each node of a regularly spaced, three-dimensional grid constituting the inversion grid. The inversion was carried out using a nonlinear minimum approach based on a stochastic description of the data and the model.

Using arrival times from our catalog augmented by data from the Centro Sismológico Nacional (CSN) for the period from 2000 to 2017, we built a local V_P and V_P/V_S tomographic model for the MP bounded

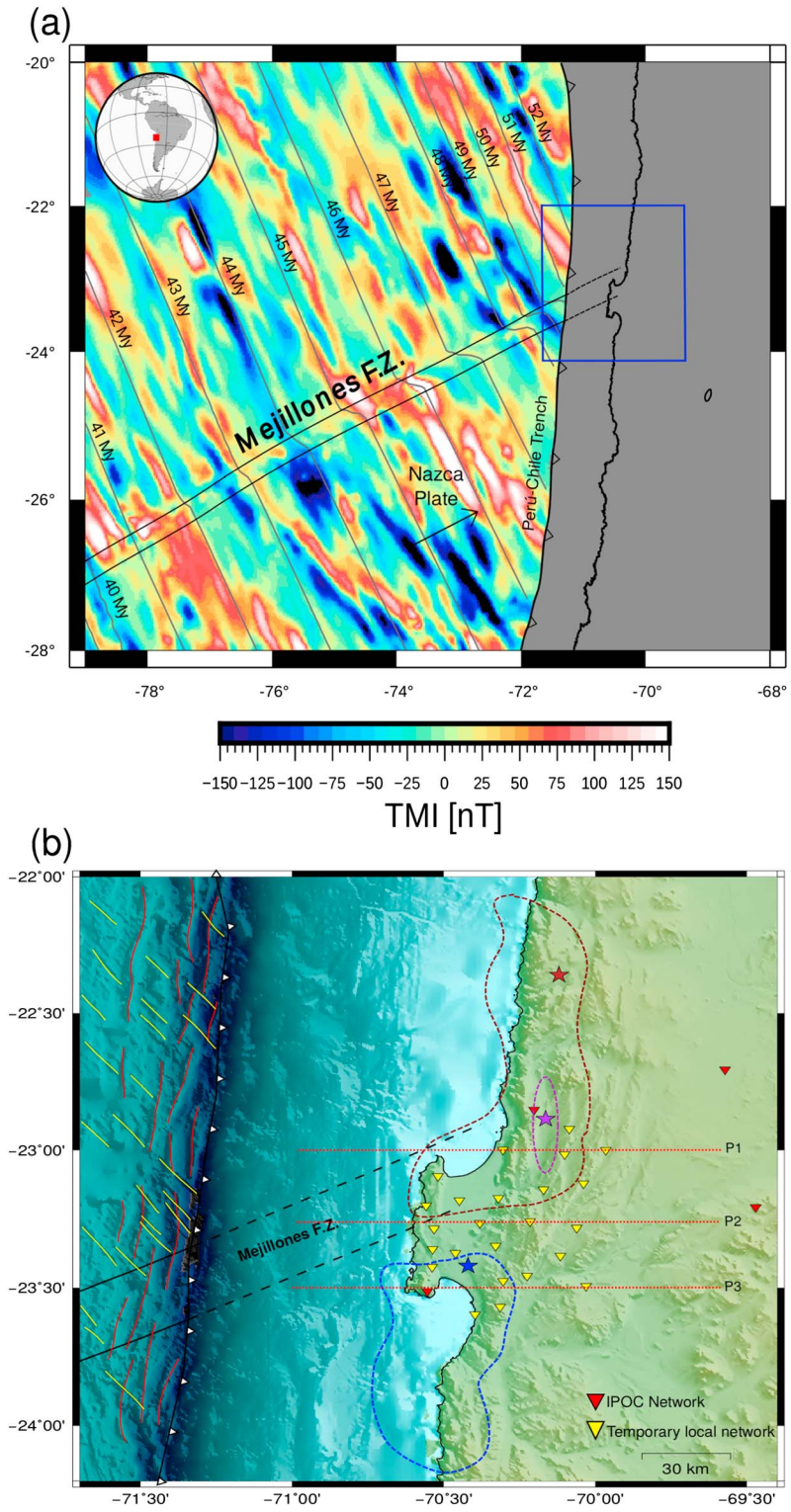

Figure 1. Seismotectonic setting of the Mejillones Peninsula. (a) Oceanic magnetic lineament corresponding to the Mejillones fracture zone. Colored images are the total magnetic intensity of the oceanic Nazca plate according to the 2-arc-minute-resolution Earth Magnetic Anomaly satellite geomagnetic field. Gray lines are the interpolated iso-contours of the slab age (Müller et al., 2008). (b) Inverted yellow and red triangles corresponding to the seismological networks used. Brown, blue, and purple dashed lines are the ruptures, and stars are the epicenters of the 2007 Tocopilla, 1995 Antofagasta, and 2007 Michilla earthquakes, respectively. Red and yellow solid lines correspond to the faults in the outer-rise region. Red dashed lines correspond to the 3-D tomographic profiles presented in Figure 3.

approximately from 22.8°S to 24.2°S and from 69.2°W to 71.2°W. The model was derived from the arrival times of 80,078 *P* waves and 79,806 *S* waves corresponding to 31,598 events in an inversion grid constituted by 1,514,394 grid cells with longitudinal, latitudinal, and vertical resolution sizes of 2 km, 2 km, and 1 km, respectively.

3. Results

3.1. Interplate Seismicity

The interplate seismicity (gray dots in Figure 2a) is concentrated toward the offshore region, and it decreases considerably onshore (Figure 2a). This absence of seismicity along the interface coincides with a shallower downdip region under the MP with an approximate depth of 32 km (Figure 2c). The depth of updip seismicity varies between 22 and 25 km depth. Most of the focal mechanisms indicate reverse faults with low-angle nodal planes that coincide with the dip angle of the subduction (Figures 2b–2d). This distinctive pattern in the seismicity, in conjunction with aseismic pulses (Pritchard & Simons, 2006) suggests that the interface under the MP presents a stable frictional behavior. The shallower downdip region under the MP could be interpreted as a shallower seismogenic zone (Schurr et al., 2012). This pattern in the distribution of seismicity was also observed in the aftershocks of the Antofagasta and Tocopilla earthquakes around the MP (Nippress & Rietbrock, 2007; Schurr et al., 2012) and in the seismicity recorded by the IPOC network (Sippl et al., 2018). Therefore, this seismic gap is a persistent feature lasting at least since the start of the seismic record.

3.2. Intraslab Seismicity

The intraslab seismicity (red dots in Figure 2a) is concentrated toward the northern MP and it decreases toward the south. This spatial distribution could be related to the presence of the MFZ in the central and northern MP. However, part of the intraslab seismicity distribution follows north-south and northwest-southeast orientations that are correlated with the structural trends of outer-rise bend faults at the latitude of the MP. (Ranero et al., 2005). The north-south set in the outer-rise (red lines in Figure 1b) forms prominent horst and graben structures that are oriented parallel to the trench and are related to the bending of the incoming plate, while the northwest set, which is generally less pervasive (yellow lines in Figure 1b) constitutes faults formed in the center of expansion that are reactivated in the outer-rise. These faults reactive during subduction and probably generate intraslab seismicity, highlighting the long-term permanence of the outer-rise faulting during the subduction process. The focal mechanisms indicate that these faults are reactivated as reverse faults (Figures 2b–2d) whose nodal planes indicate vertical or subvertical ruptures.

3.2.1. Persistent Intraslab Seismicity

This seismicity corresponds to the Michilla cluster (Figures 2a and 2b), which likely represents aftershocks in the rupture zone of the Michilla Mw 6.7 earthquake that occurred on 16 December 2007 (Fuenzalida et al., 2013; Ruiz & Madariaga, 2011; Figure 1b). This cluster stretches from the top to the base of the oceanic crust. To confirm this, we utilized two events from the cluster that occurred at the top and the base of the crust and compared the *P* and *S* waves arrival times on the vertical components. The difference of 1 second between the *P* and *S* waves for both events (Figure S4) is equivalent to a vertical difference of approximately 8 km, which suggests that the Michilla cluster affects the entire oceanic crust. Even eight years after the Michilla earthquake, the same rupture zone is still active with abundant seismicity.

3.3. Seismicity of the Continental Crust

Seismicity within the continental crust is scarce. We found clusters that corresponded to blasting activity associated with mining in the area (brown dots in Figure 2a). To differentiate blasting events from tectonic events, we eliminated those events within the blast schedules of the mining companies (between 9 am and 9 pm local time). The result was a total of 87 tectonic events (yellow dots in Figure 2a). Some of the focal mechanisms are normal, which is consistent with the geological extensional regime of the area (Allmendinger & González, 2009).

The most striking structure is the streak that extends from the 33 km depth from the interface to the upper crust, at the downdip limit of the seismicity (Figure 2b). The focal mechanisms of these events are variable with normal, reverse and certain oblique components (Figure 2b). An explanation for this streak of seismicity could be that fluids migrate from the subducted dehydrated oceanic crust to the continental crust through

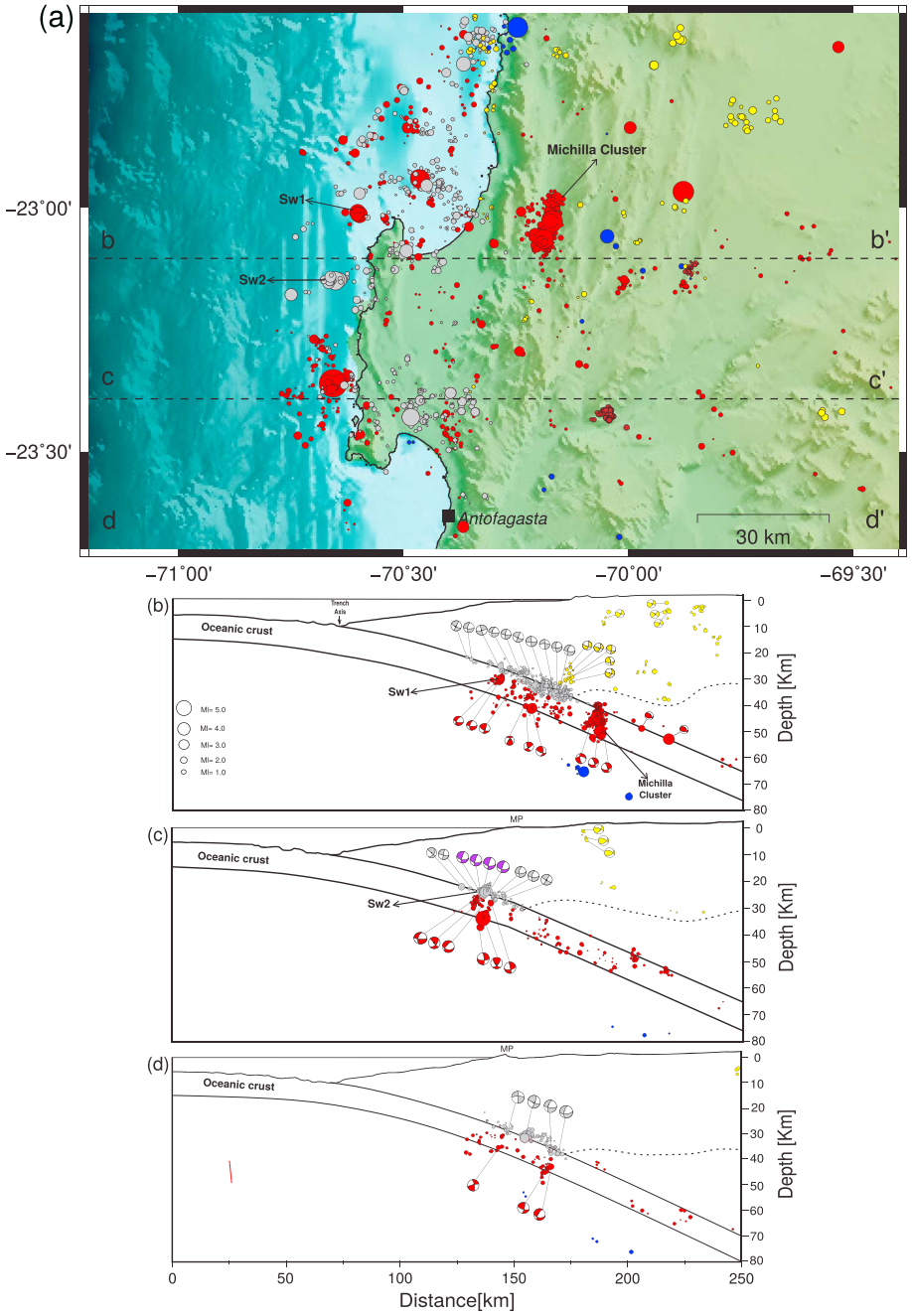

Figure 2. Seismicity and focal mechanisms. (a) Plan view of the seismicity. Gray circle: interplate seismicity; red: intraslab seismicity; yellow: continental crust seismicity; blue: upper oceanic mantle seismicity; and brown: mining activity seismicity. Sw1 and Sw2 correspond to swarms with repeaters. The colors of the focal mechanisms correspond to the colors of the seismicity; purple corresponds to swarm Sw2. (b) Events from b-b′ to the north, (c) events between b-b′ and c-c′, and (d) events between c-c′ and d-d′. From (b) to (d) the dashed line represents the intersection between the mantle wedge and the plate interface.

preexisting fracture zones, which generally have a higher permeability, thereby facilitating the channeling of fluids that trigger seismicity (Nakajima & Uchida, 2018; Nippress & Rietbrock, 2007).

3.4. Swarms and Repeaters

We were able to recognize two swarms. The first (Sw1 in Figures 2a and 2b) occurred inside the oceanic crust, with a total of 14 events, and it lasted approximately 1 month. The second (Sw2 in Figures 2a and 2c) occurred

at the plate interface and lasted 12 days with a total of 42 events. Analyzing these swarms in more detail, we noticed the presence of repeaters among the events that compose the swarms. The repeaters were identified by the coherence of the vertical component throughout the record in the frequency band from 2 to 8 Hz (Obara, 2011). A repeater was defined when the correlation coefficient in two or more stations exceeded 0.95 (Uchida & Matsuzawa, 2013). We found a total of 2 repeaters for Sw1 and 32 for Sw2, each repeater was identified in more than three stations, with the exception of the Sw1 repeaters, which were identified with only two stations (Figure S5).

3.5. 3-D Tomography

3.5.1. Continental Crust

The *P* wave velocities fluctuated between 5 and 6.5 km/s in the shallow continental crust (<15 km) and did not present an along-strike variation. An area with low velocities (V_P ~ 4 to 4.5 km/s) is observed along profile 3b at depths between 0 and 4 km; this anomaly could correspond to the sediments of the Mejillones basin. This behavior changes in the lowermost upper crust (>15 km), where the V_P varies along-strike. To the north and in the center of the MP, there is an increase in the V_P with values from 7.0 to 7.2 km/s just above the top of the oceanic crust (Figures 3a and 3b), while it decreases to <7.0 km/s to the south (Figure 3c).

The V_P/V_S values vary along-strike in the shallow upper crust (<15 km) reaching values between 1.74 and 1.68. In contrast in the lowermost upper crust (~15–35 km), high V_P/V_S values fluctuating between 1.80 and 1.86 stand out toward the north and in the center of MP (Figures 3d and 3e). Finally, to the south of the MP, the V_P/V_S values decrease sharply to 1.74 and 1.68 at the same depth (Figure 3f).

3.5.2. Oceanic Crust

The *P* waves velocities in the oceanic crust vary along-strike. Toward the north and in the center of the MP, the *P* waves velocities increase to values ranging from 7.2 to 7.5 km/s (Figures 3a and 3b), while to the south, they decrease to values ranging from 6.8 to 7.0 km/s (Figure 3c).

The V_P/V_S values in the oceanic crust are high, reaching between 1.82 to 1.86 toward the north and in the center of the MP (Figures 3d and 3e) and between 1.78 to 1.80 toward the south (Figure 3f). These high values are concentrated further updip, while they decrease in the downdip direction (see Figures S6 to S8 for the resolution and quality of the results).

4. Interpretation and Discussion

4.1. Hydration in the Oceanic Crust

The V_P and V_P/V_S values in the oceanic crust are higher than the expected values of basalt and gabbros (Christensen, 1996). We associate these high values with hydrated zones due to fluids released by progressive metamorphic dehydration reactions within the subducted oceanic crust (Hacker et al., 2003; Kato et al., 2010; Peacock, 2001). These zones rich in fluids have a direct association with the distributions of the intraslab seismicity, swarms, and repeaters (Figures 3d, 3e, and 3f). The fluids released into the oceanic crust weaken preexisting faults and trigger intraslab seismicity (Kirby et al., 1996; Rietbrock & Waldhauser, 2004). While the swarms and repeaters are more likely to occur in subduction zones with abundant fluids, with marked heterogeneity on the plate interface and indicate the activation of hydrated fractures (Nishikawa & Ide, 2017; Poli et al., 2017). The hydration in the oceanic crust varies along-strike, and it is more pronounced toward the north and in the center of the MP. Nishikawa and Ide (2015) postulated that greater bending in the subducting plate causes more faulting in the outer-rise zone, thereby increasing the hydration of the oceanic crust, which finally leads to additional dehydration and an increase in the pore-fluid pressure. Other studies concluded that latitudinal variations in hydration are caused by the subduction of hydrated fracture zones present within the oceanic crust (Moreno et al., 2014; Poli et al., 2017). The fracture zones are recognized as important fluid sinks capable of producing a significant and localized lateral variation in the amount of fluids, that is, the fracture zones, with greater permeability, transport much more fluid to the subduction zone (Moreno et al., 2014). The high intensity of hydration in the oceanic crust to the north of the MP correlates with the MFZ, which is being subducted under the MP (Figure 1). We suggest that the greater degree of hydration in the oceanic crust to the north of the MP is due to the subduction of the MFZ, thereby causing the additional release of fluid in this area. This is also reflected in the observed seismicity; the most hydrated areas have a higher rate of seismicity during the interseismic period (Schlaphorst et al., 2016).

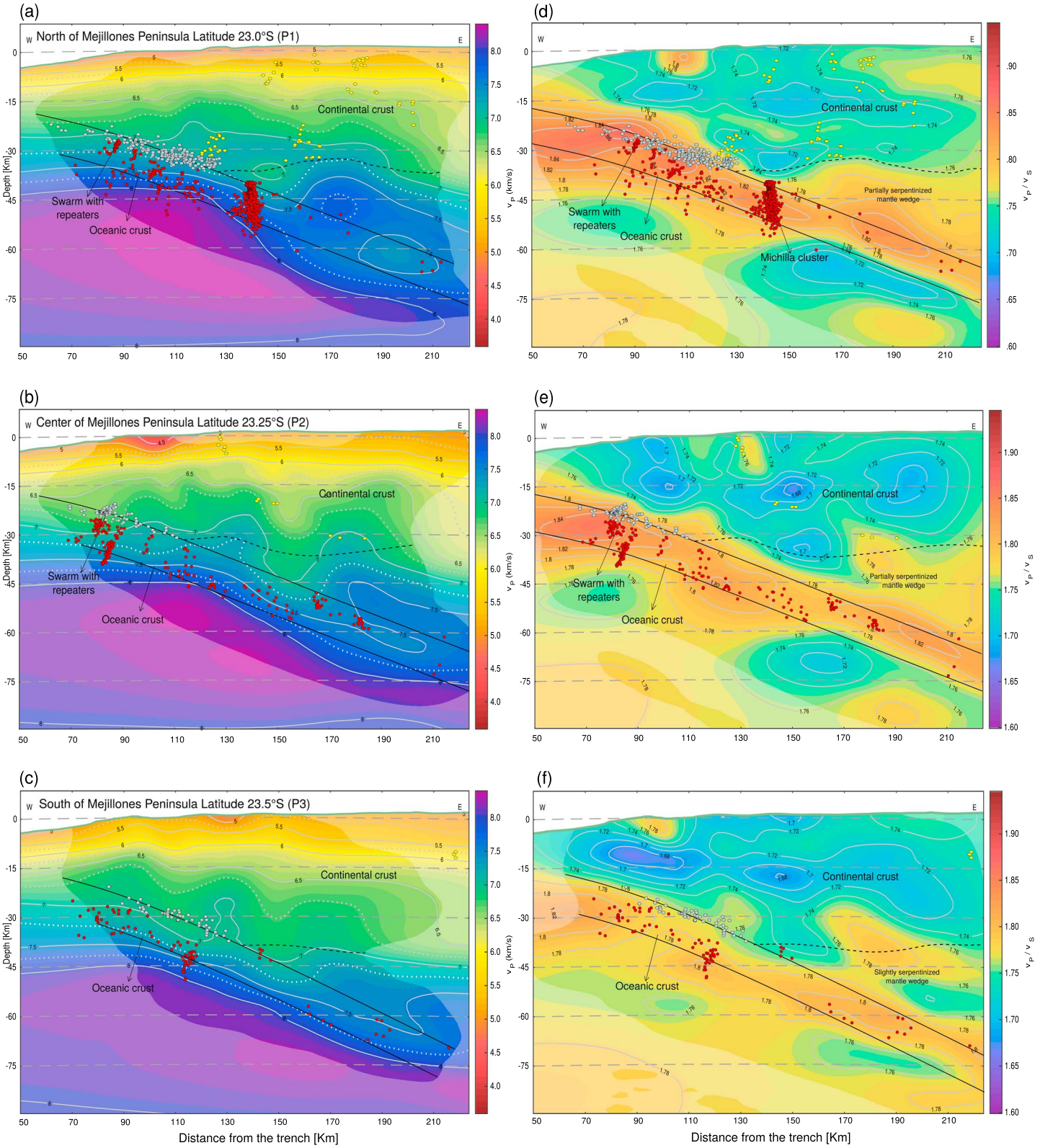

Figure 3. The 3-D tomography model. Black solid line represents subducted oceanic crust, black dashed line represents the continental Moho, and less illuminated areas represent zones without resolution. Panels (a)–(c) show the *P* wave velocities; panels (d)–(f) show the V_P/V_S ratio for the northern, central, and southern Mejillones Peninsula, respectively (red dashed lines in Figure 1b). Gray, red, and yellow dots are the interplate, intraslab, and continental crust seismicity, respectively.

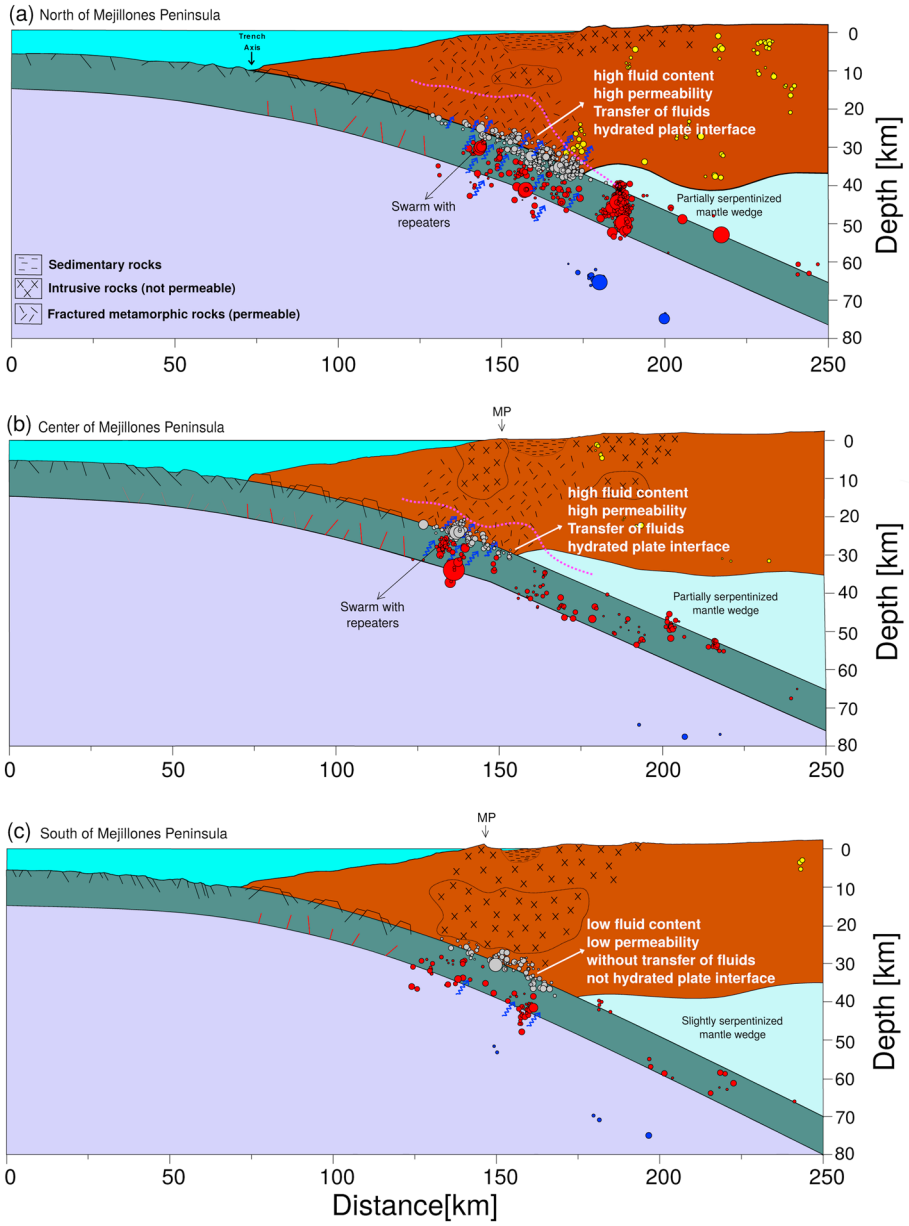

Figure 4. Schematic diagram of the hydration and seismicity. Blue arrows denote potential fluid pathways along the plate interface. The black lines represent horsts and grabens in the outer-rise that are subsequently subducted. Red lines are reactivated faults inside the oceanic crust. Panels (a) and (b) are the northern and central profiles of the Mejillones Peninsula (23°S and 23.25°S) with high concentrations of seismicity, swarms, repeaters, and fluids. The fractured and permeable rocks in the upper crust allow the passage of fluids causing high fluid content at the plate interface. (c) Southern profile of the Mejillones Peninsula (23.5°S), with a low seismicity, no swarms, and fewer fluids. The impermeable intrusive rocks of the upper crust prevent the passage of fluids, causing a lower fluid content at the plate interface.

4.2. Hydration in the Continental Crust

The V_P and V_P/V_S values in the shallow parts of the continental crust (<15 km) are associated with metamorphic and intrusive rocks (Christensen, 1996). Metamorphic rocks show V_P/V_S values between 1.74 and 1.76, while intrusive rocks have values ranging from 1.68 to 1.72. Upon observing the distribution of the V_P/V_S ratio (Figures 3d, 3e, and 3f) metamorphic rocks evidently predominate toward the north and in the center of the MP, while dioritic intrusive rocks predominate toward the south, which is consistent with the near surface geology (Figure S9a). This pattern changes in the lower part of the continental crust (~15–35 km), just above the top of the hydrated oceanic crust. The high V_P/V_S values between 1.80 and

1.86 toward the north and in the center of the MP (Figures 3d and 3e) are higher than those of metamorphic rocks in the sector (Hacker et al., 2003). The most suitable lithology that presents similar V_P/V_S values is serpentinite, specifically the species lizardite (Christensen, 1996, 2004); however, at shallow depths (25–45 km) serpentinite does not appear in sufficiently high quantities to alter the V_P/V_S ratio in the observed way. These high V_P/V_S values in the lower upper crust can be interpreted as fluid-rich metamorphic rocks (Peacock et al., 2011). This situation is not observed to the south of the MP (Figure 3f), and the V_P/V_S values between 1.68 and 1.72 remain consistent with the dioritic intrusive rocks of that sector.

The existence of areas that are enriched with fluids inside the lower continental crust implies that fluids were able to migrate into the continental crust. If the geology of the continental crust is uniform in terms of its porosity and permeability, the distribution of fluids therein should also be uniform. However, in the MP the fluid distributions are not uniform, and neither is the geology. Zhang (2013) and Lamur et al. (2017) through experimental methods in intact and fractured rocks, postulate that fractured metamorphic rocks such as those present toward the north and in the center of MP, have a higher permeability (~10^{-10} to 10^{-13} m^2) in contrast, to the south, intrusive dioritic, and granitic rocks are not fractured and have a lower permeability (~10^{-17} to 10^{-19} m^2). The distribution of areas with a high fluid content in the lowermost upper crust correlates with the change in lithology within the continental crust. The fractured and permeable rocks to the north and in the center of the MP allow the passage of fluids from the hydrated oceanic crust toward the upper crust producing high fluid content in the lower part of the continental crust. However, the unfractured and impermeable rocks to the south of the MP impede the passage of fluids toward the upper crust (Figure 4).

4.3. Hydration and Interseismic Coupling

The transfer of fluids from oceanic crust to continental crust observed to the north and in the center of the MP suggests a more hydrated plate interface, which is spatially correlated with the zones of low coupling and the MFZ under the MP (Metois et al., 2016; Figure S9b). In contrast to the south of the MP, because there is no fluid transfer, we infer a less hydrated plate interface that correlates with zones of high coupling and the regular occurrence of megathrust earthquakes (e.g., the 1995 Mw 8.1 Antofagasta earthquake). Therefore, we suggest that the areas of low coupling under the MP are due to the presence of a hydrated MFZ and fluids along the plate interface, favoring creep or aseismic slip, which is similar to hypothesis of Moreno et al. (2014) for the southern Arauco Peninsula.

5. Conclusion

We studied the seismogenic behavior of the subduction zone under the MP, through an analysis of seismicity data and the construction of a 3-D tomographic model. In the northern and central MP, a more hydrated oceanic crust associated with the presence of the MFZ and permeable rocks in the continental crust, allows a higher fluid concentration at the plate interface. Consequently, this region presents a high rate of seismicity with low coupling, in addition to swarms, repeaters and it acts as a seismic barrier to the propagation of the rupture of megathrust earthquakes. In contrast, in the southern region of the MP, a less hydrated oceanic crust and impermeable rocks in the continental crust prevent fluid accumulation and favor a lower fluid content along the plate interface, causing a high degree of coupling and a low rate of seismicity, without swarms or the occurrence of regular megathrust earthquakes. We conclude that the seismogenic behavior of the subduction zone beneath the MP is controlled by differences in the fluid distribution, particularly highlighting the role of the lithology of the continental crust and its physical properties in the distribution of fluids along the plate interface. Our results are important for prospective future analyses of earthquake distributions and hazard assessments.

Acknowledgments
This work was funded by the Fondap CIGIDEN project 15110017. We thank the GeoForshungszentrum Potsdam and the Freie Universität Berlin for providing the seismological stations and the CSN, Centro Sismológico Nacional, for providing us the seismic catalog. S. R. and A. M. thank Conicyt PIA/Anillo grant ACT172002. The waveforms of the temporary stations used in this study MEJIPE seismic network (https://doi.org/10.7914/SN/8G_2013; Salazar et al., 2013) are currently restricted and are not currently available for the rest of the scientific community. While the data provided by the Centro Sismológico Nacional (CSN) are freely accessible as well as the freely accessible IPOC data for the community available on the GEOFON website. We used the Generic Mapping Tool (http://gmt.soes.hawaii.edu/) and other free software to prepare the manuscript figures.

References

Allmendinger, R. W., & González, G. (2009). Neogene to quaternary tectonics of the coastal Cordillera, northern Chile. *Tectonophysics*, *495*(1-2), 93–110. https://doi.org/10.1016/j.tecto.2009.04.019

Audet, P., & Schwartz, S. Y. (2013). Hydrologic control of forearc strength and seismicity in the Costa Rican subduction zone. *Nature Geoscience*, *6*(10), 852–855. https://doi.org/10.1038/ngeo1972

Bejar-Pizarro, M., Socquet, A., Armijo, R., Carrizo, D., Genrich, J., & Simons, M. (2013). Andean structural control on interseismic coupling in the North Chile subduction zone. *Nature Geoscience*, *6*(6), 462–467. https://doi.org/10.1038/ngeo1802

Christensen, N. I. (1996). Poisson's ratio and crustal seismology. *Journal of Gephysical Research*, *101*(B2), 3139–3156. https://doi.org/10.1029/95JB03446

Christensen, N. I. (2004). Serpentinites, peridotites, and seismology. *International Geology Review*, *46*(9), 795–816. https://doi.org/10.2747/0020-6814.46.9.795

Comte, D., & Pardo, M. (1991). Reappraisal of great historical earthquakes in the northern Chile and southern Peru seismic gaps. *Natural Hazards*, *4*(1), 23–44. https://doi.org/10.1007/BF00126557

Delouis, B., Monfret, T., Dorbath, L., Pardo, M., Rivera, L., Comte, D., et al. (1997). The Mw = 8.0 Antofagasta (northern Chile) earthquake of 30 July 1995: A precursor to the end of the large 1877 gap. *Bulletin of the Seismological Society of America*, *87*(2), 4–27.

Delouis, B., Pardo, M., Legrand, D., & Monfret, D. (2009). The Mw 7.7 Tocopilla earthquake of 14 November 2007 at the southern edge of the northern Chile seismic gap: Rupture in the deep part of coupled plate interface. *Bulletin of the Seismological Society of America*, *99*(1), 87–94. https://doi.org/10.1785/0120080192

Fuenzalida, A., Schurr, B., Lancieri, M., Sobiesiak, M., & Madariaga, R. (2013). High-resolution relocation and mechanism of aftershocks of the 2007 Tocopilla (Chile) earthquake. *Geophysical Journal International*, *194*, 1216–1228.

González, G., Salazar, P., Loveless, J. P., Allmendinger, W., Aron, F., & Shrivastava, M. (2015). Upper plate reverse fault reactivation and the unclamping of the megathrust during 2014 northern Chile earthquake sequence. *Geology*, *43*(8), 671–674. https://doi.org/10.1130/G36703.1

Hacker, B. R., Peacock, S. M., Abers, G. A., & Holloway, S. D. (2003). Subduction factory 2. Are intermediate-depth earthquakes in subducting slabs linked to metamorphic dehydration reactions? *Journal of Geophysical Research*, *108*(B1), 2030. https://doi.org/10.1029/2001JB001129

Havskov, J., & Ottemöller, L. (Eds.) (2000). *SEISAN: The earthquake analysis software for Windows, SOLARIS, LINUX and MACKINTOSH version 8.2. Manual*. Norway: Department of Earth Science, University of Bergen.

Husen, S., Kissling, E., Flueh, E., & Asch, G. (1999). Accurate hypocentre determination in the seismogenic zone of the subducting Nazca Plate in northern Chile using a combined on-/offshore network. *Geophysical Journal International*, *138*(3), 687–701. https://doi.org/10.1046/j.1365-246x.1999.00893.x

IPOC (2006). IPOC Seismic Network, Integrated Plate Boundary Observatory Chile. https://doi.org/10.1447/PK615318.Other/seismicnetwork

Kato, A., Iidaka, T., Ikuta, R., Yoshida, Y., Katsumata, K., Iwasaki, T., et al. (2010). Variations of fluid pressure within the subducting oceanic crust and slow earthquakes. *Geophysical Research Letters*, *37*, L14310. https://doi.org/10.1029/2010GL043723

Kirby, S., Engdahl, E. R., & Denlinger, R. (1996). Intermediate-depth intraslab earthquakes and arc volcanism as physical expressions of crustal and uppermost mantle metamorphism in subducting slabs. In *Subduction: Top to bottom, Geophysical Monograph*, 96 (pp. 195–214).

Lamur, A., Kendrick, J. E., Eggertsson, G. H., Wall, R. J., Ashworth, J. D., & Lavallée, Y. (2017). The permeability of fractured rocks in pressurised volcanic and geothermal system. *Nature Scientific Reports*, *7*(1), 6173. https://doi.org/10.1038/s41598-017-05460-4

Lomax, A. J., Virieux, P., Volant, P., & Berge, C. (2000). Probabilistic earthquake location in 3D and layered model: Introduction of a Metropolis-Gibbs method and comparison with linear location. In C. H. Thurber & N. Rabinowitz (Eds.), *Advances in Seismic Event Location* (pp. 101–134). Amsterdam: Springer. https://doi.org/10.1007/978-94-015-9536-0_5

Maksymowicz, A. (2015). The geometry of the Chilean continental wedge: Tectonic segmentation of subduction processes off Chile. *Tectonophysics*, *659*(2015), 183–196. https://doi.org/10.1016/j.tecto.2015.08.007

Metois, M., Vigny, C., & Socquet, A. (2016). Interseismic coupling, megathrust earthquake and seismic swarms along the Chilean subduction zone. *Pure and Applied Geophysics*, *173*, 1431–1449.

Moreno, M., Haberland, C., Oncken, O., Rietbrock, A., Angiboust, S., & Heidbach, O. (2014). Locking of the Chile subduction zone controlled by fluid pressure before the 2010 earthquake. *Nature Geoscience*, *7*(4), 292–296. https://doi.org/10.1038/ngeo2102

Müller, R. D., Sdrolias, M., Gaina, C., & Roest, W. R. (2008). Age, spreading rates and spreading symmetry of the world's ocean crust. *Geochemistry, Geophysics, Geosystems*, *9*, Q04006. https://doi.org/10.1029/2007GC001743

Nakajima, J., & Uchida, N. (2018). Repeated drainage from megathrusts during episodic slow slip. *Nature Geoscience*, *11*(5), 351–356. https://doi.org/10.1038/s41561-018-0090-z

Nippress, S. E. J., & Rietbrock, A. (2007). Seismogenic zone high permeability in the central Andes inferred from relocations of micro-earthquakes. *Earth and Planetary Science Letters*, *263*(3-4), 235–245. https://doi.org/10.1016/j.epsl.2007.08.032

Nishikawa, T., & Ide, S. (2015). Background seismicity rate at subduction zones linked to slab-bending-related-hydration. *Geophysical Research Letters*, *42*, 7081–7089. https://doi.org/10.1002/2015GRL064578

Nishikawa, T., & Ide, S. (2017). Detection of earthquake swarms at subduction zones globally: Insight into tectonic controls on swarm activity. *Journal of Geophysical Research: Solid Earth*, *122*, 5325–5343. https://doi.org/10.1002/2017JB014188

Obara, K. (2011). Characteristics and interactions between non-volcanic tremor and related slow earthquakes in the Nankai subduction zone, southwest Japan. *Journal of Geodynamics*, *52*(3-4), 229–248. https://doi.org/10.1016/j.jog.2011.04.002

Peacock, S. M. (2001). Are the lower planes of double seismic zones caused by serpentine dehydration in subducting oceanic mantle? *Geology*, *29*(4), 299–302. https://doi.org/10.1130/0091-7613(2001)029<0299:ATLPOD>2.0.CO;2

Peacock, S. M., Christensen, N. I., Bostock, M. G., & Audet, P. (2011). High pore pressures and porosity at 35 km depth in the Cascadia subduction zone. *Geology*, *39*(5), 471–474. https://doi.org/10.1130/G31649.1

Peyrat, S., Madariaga, R., Buforn, E., Campos, J., Asch, G., & Vilotte, J. P. (2010). Kinematic rupture process of the 2007 Tocopilla earthquake and its main aftershocks from teleseismic and strong motion data. *Geophysical Journal International*, *182*(3), 1411–1430. https://doi.org/10.1111/j.1365-246X.2010.04685.x

Poli, P., Maksymowicz, A., & Ruiz, S. (2017). The Mw 8.3 Illapel earthquake (Chile): Preseismic and postseismic activity associated with hydrated slab structures. *Geology*, *45*(3), 247–250. https://doi.org/10.1130/G38522.1

Potin, B. (2016). Les Alpes Occidentales: Tomographie, localisation de séismes et topographie du Moho, PhD *thesis, University Grenoble-Alpes (France), ISTerre*.

Pritchard, M. E., & Simons, M. (2006). An aseismic slip pulse in northern Chile and along-strike variations in seismogenic behavior. *Journal of Geophysical Research*, *111*, B08405. https://doi.org/10.1029/2006JB004258

Ranero, C. R., Villaseñor, A., Morgan, J. P., & Weinrebe, W. (2005). Relationship between bend-faulting at trenches and intermediate-depth seismicity. *Geochemistry, Geophysics, Geosystems*, *6*, Q12002. https://doi.org/10.1029/2005GC000997

Rietbrock, A., & Waldhauser, F. (2004). A narrowly spaced double-seismic zone in the subducting Nazca plate. *Geophysical Research Letters*, *31*, L10608. https://doi.org/10.1029/2004GL019610

Ruiz, S., & Madariaga, R. (2011). Determination of the friction law parameters of the Mw 6.7 Michilla earthquake in northern Chile by dynamic inversion. *Geophysical Research Letters*, *38*, L09317. https://doi.org/10.1029/2011GRL047147

Ruiz, S., & Madariaga, R. (2018). Historical and recent large megathrust earthquakes in Chile. *Tectonophysics*, *733*(2018), 37–56. https://doi.org/10.1016/j.tecto.2018.01.015

Ruiz, S., Metois, M., Fuenzalida, A., Ruiz, J., Leyton, F., Grandin, R., et al. (2014). Intense foreshocks and slow slip event preceded the 2014 Iquique Mw 8.1 earthquake. *Science*, *345*(6201), 1165–1169. https://doi.org/10.1126/science.1256074

Salazar, P., Wigger, P., Bloch, W., Asch, G., Shapiro, S. A., & Kummeorw, J. (2013). MEJIPE. International Federation of Digital Seismograph Networks. *Other/Seismic Network*. https://doi.org/10.7914/SN/8G_2013

Schlaphorst, D., Kendall, J., Collier, J., Verdon, J., Blundy, J., Baptie, B., et al. (2016). Water, oceanic fracture zones and the lubrication of subducting plate boundaries-insights from seismicity. *Geophysical Journal International*, *204*(3), 1405–1420. https://doi.org/10.1093/gji/ggv509

Schurr, B., Asch, G., Hainzl, S., Bedford, J., Hoechner, A., Palo, M., et al. (2014). Gradual unlocking of plate boundary controlled initiation of the 2014 Iquique earthquake. *Nature*, *512*(7514), 299–302. https://doi.org/10.1038/nature13681

Schurr, B., Asch, G., Rosenau, M., Wang, R., Oncken, O., Barrientos, S., et al. (2012). The 2007 M7.7 Tocopilla northern Chile earthquake sequence: Implications for along-strike and downdip rupture segmentation and megathrust frictional behavior. *Journal of Geophysical Research*, *117*, B05305. https://doi.org/10.1029/2011JB009030

Sippl, C., Schurr, B., Asch, G., & Kummerow, J. (2018). Seismicity structure of the northern Chile forearc from >100,000 double-difference relocated. *Journal of Geophysical Research: Solid Earth*, *123*, 4063–4087. https://doi.org/10.1002/2017JB015384

Snoke, J. A., Munsay, J. W., Teague, A. G., & Bollinger, G. A. (1984). A program for focal mechanism determination by combined use of polarity and SV-P amplitude ratio data. *Earth Notes*, *55*(3), 15.

Uchida, N., & Matsuzawa, T. (2013). Pre- and postseismic slow slip surrounding the 2011 Tohoku-oki earthquake rupture. *Earth and Planetary Science Letters*, *374*, 81–91. https://doi.org/10.1016/j.epsl.2013.05.021

Waldhauser, F., & Ellsworth, W. L. (2000). A double-difference earthquake location algorithm: Method and application to the northern Hayward fault, California. *Seismological Society of America Bulletin*, *90*(6), 1353–1368. https://doi.org/10.1785/0120000006

Zhang, L. (2013). Aspects of rock permeability. *Frontiers of Structural and Civil Engineering*, *7*(2), 102–116. https://doi.org/10.1007/s11709-013-0201-2